Surface Characteristics of Ti/IrO$_2$ Anode Material and its Electrocatalytic Properties for Polycyclic Aromatic Hydrocarbons (PAHs) Degradation in Aqueous Solution

Asim Yaqub[1,*], Mohamed Hasnain Isa[1], Shamsul Rahman Mohamed Kutty[1] and Huma Ajab[2]

[1]Civil Engineering Department, Universiti Teknologi PETRONAS, Bandar Seri Iskandar 31750 Tronoh, Perak, Malaysia
[2]Chemical Engineering Department, Universiti Teknologi PETRONAS, Bandar Seri Iskandar 31750 Tronoh, Perak, Malaysia

Abstract: *In this study, electrochemical degradation of 16 priority PAHs was examined using Ti/IrO$_2$ anode. Iridium dioxide (IrO$_2$) was coated by thermal decomposition of appropriate precursor solution on surface of titanium plate. Surface morphology of coated surface was observed by FESEM and XRD analysis. All electrochemical experiments were conducted using synthetic solution of PAHs in a batch cell under galvanostatic condition. GC-MS was used to quantify PAHs concentration. Electrochemical oxidation results reveal significant degradation of PAHs at Ti/IrO$_2$ surface. Total PAHs removal was about 97 % at all studied initial pH values 3, 6 and 9 in the presence of electrolyte. Crystalline surface of Ti/IrO$_2$ anode exhibited good electrocatalytic properties towards PAHs degradation.*

1. INTRODUCTION

Polycyclic aromatic hydrocarbons (PAHs) are common organic pollutants in air, soil and water. They consist of two or more fused benzene rings containing only carbon and hydrogen. PAHs are released into atmosphere through forest fires, volcanic eruptions and through vehicle exhausts. Soil and water are contaminated by PAHs through oil spills, produced water discharge, urban runoff, domestic and industrial wastewater discharges. PAHs are among the group of compounds defined as persistent organic pollutants. Discovery of the carcinogenic properties of benzo(α)pyrene in the 1930s first stimulated interest in PAH chemistry. Since then many PAHs have been identified as potent carcinogens and mutagens, and the United States Environmental Protection Agency (USEPA) has designated 16 PAHs as priority pollutants [1]. These PAHs, considered as a group, have been identified as being of greatest concern with regard to potential exposure and adverse health effects on humans [2]. Characteristics of 16 priority PAHs are given in Table 1.

Several technologies have been developed to treat PAH contaminated soils and sludge [5-7]. Very few studies have reported the treatment of PAHs contaminated water. Biological treatment using bacteria, fungi and algae have been applied to degrade a

range of low molecular weight PAHs, such as naphthalene, fluorene and phenanthrene; however, their activity towards high molecular weight PAHs containing five or more fused benzene rings, such as Benzo(a)pyrene and Benzo(ghi)perylene, is limited [8].

Electrochemical treatment of wastewater has attracted wide attention as one of the environmentally-friendly technologies [9, 10]. The active coating materials of electrodes are very important for pollutants degradation in electrochemical oxidation process. Some researchers showed that coated titanium anode plates exhibited good effect on electrochemical oxidation and wastewater treatment [11].

Iridium dioxide (IrO$_2$) belongs to the family of transition-metal dioxides found in its rutile structure at ambient pressure with a metallic behavior [12]. It shows high chemical and thermal stability [13]. IrO$_2$ based dimensionally stable anodes (DSA) are known to be good electro-catalysts; they present excellent electrocatalytic properties and good stability in strong acid solution for chlorine and oxygen evolution [14-17]. They can generate hydroxyl radicals and active chlorine species to destroy refractory organic wastes into carbon dioxide [18, 19].

Coating of IrO$_2$ on titanium surface could enhance the stability and prolong the life of electrodes [20-23]. Due to its stability and longer life time, IrO$_2$ electrode has attracted a lot of attention in commercial application of Dimensionally Stable Anodes (DSAs) [24].Due to the presence of an IrO$_2$ interlayer increase in service

*To whom correspondence should be addressed:
Email: environment_green@yahoo.com Phone: +6053687346, Fax: +6053656217

life of Ti/SnO$_2$–Sb$_2$O$_5$ electrodes were reported during electrochemical oxidation of p-chlorophenol [25], salicylic acid and salicylaldehyde [26] and decolorization of methyl orange dye at IrO$_2$-SnO$_2$-Sb$_2$O$_5$ [27].

In order to achieve better application of electrochemical oxidation process, IrO$_2$ was coated on titanium plate and used as anode for PAHs degradation. In this study, electrocatalytic activity of Ti/IrO$_2$ material for PAHs degradation in water was investigated.

2. MATERIALS AND METHODS

2.1. Anode coating

Pretreated titanium plates were coated with IrO$_2$ by thermal decomposition method [28]. Precursor solutions were prepared from the following analytical grade reagents: citric acid (CA), ethyleneglycol (EG), and iridium chloride IrCl$_3$.xH$_2$O in ratio of CA: EG: IrCl$_3$.xH$_2$O (2ml: 10ml: 0.1 g) were dissolve at 60 °C for 1 hr.

Rectangular Ti plates (8 cm × 1 cm × 0.2 cm) were used as substrate for electrode preparation. The Ti plates were smoothened by 320-grit sandpaper and washed with distilled water. To remove oxides from the surface, the Ti plates were etched in 18 % HCl for 30 min at 80 °C followed by a thorough washing with deionized water. After etching, the Ti plates lost their metallic shine and their color became grey. After pretreatment, the titanium plates were coated with precursor solution at room temperature, dried at 100°C for 10 min, after 10 applications again heat treated at 450°C for 10 min. This process was repeated 3 times until the desired oxide loading and finally calcinated at 500 °C for 2h.

2.2. Electrochemical cell

All experiments were performed under galvanostatic conditions. The electrochemical cell of volume 100mL consisted of IrO$_2$ coated Ti anode (Ti/ IrO$_2$) and Ti plate cathode connected to a DC power supply. The inter-electrodes distance was 2 cm. Synthetic samples of PAHs were used in all preliminary experiments to study the effect of initial pH (3, 6 and 9) and electrolyte addition. NaCl was used as electrolyte at 1 g/L. Electrolysis time experiments was 4 h and applied current density was 3.33 mA/cm^2.

2.3. Analytical techniques

Surface morphology and Energy Dispersive Analysis of X Rays (EDAX) of coating material was observed by a Variable Pressure Field Emission Scanning Electron Microscopy (VP-FESEM) (Carl Zeiss AG, Germany Model SUPRA 55VP). X-Ray Diffraction pattern (XRD) (Bruker D8 Advance Diffractometer) was used for the crystalline structure identification of coated surface, analysis were performed at 2θ angles from 2° to 80°, with a scan speed of 4° min^{-1}.

PAHs were extracted by Liquid-Liquid Extraction Method [29, 30]. Dichloromethane DCM was used as solvent for the extraction of PAHs from water samples. Quantification of the 16 priority PAHs was performed using Gas Chromatography Mass Spectroscopy (Agilent Model GC-MS 5975C). DB 5MS column was used with dimensions of (30 m × 0.25 mm id × 0.25 μm). The column temperature was programmed from 60 to 175 °C at 6 °C/min, then increased at 3 °C/min until 240 °C and finally held at 300 °C for 7 min. Injector and transfer line temperatures were 280 and 300 °C, respectively. Data acquisition was carried out in the selected ion monitoring (SIM) mode. The PAHs standard solution was obtained from Accu-Standard and contained each of the 16 priority PAHs at concentrations of 2 mg/ml in dichloromethane/benzene. All the 16 PAHs were separately quantified using a five-point calibration of mixed standard solutions.

Table 1. Characteristics of priority PAHs [3-5]

PAHs	Abbreviation	Chemical formula	Molecular weight	Benzene rings	Solubility (mg /l)	MCL* (mg/l)	Partition coefficient (Log K$_{ow}$)
Naphthalene	Nap	C$_{10}$H$_8$	128.17	2	32 .0	-	3.37
Acenaphthylene	Acy	C$_{12}$H$_8$	152.20	3	3.93	-	4.00
Acenaphthene	Ace	C$_{12}$H$_{10}$	154.20	3	3.40	-	3.92
Fluorene	Flu	C$_{13}$H$_{10}$	166.22	3	1.90	-	4.18
Phenanthrene	Phe	C$_{14}$H$_{10}$	178.23	3	1.30	-	4.57
Anthracene	Ant	C$_{14}$H$_{10}$	178.23	3	0.07	-	4.54
Fluoranthene	Fla	C$_{16}$H$_{10}$	202.26	4	0.265	-	4.18
Pyrene	Pyr	C$_{16}$H$_{10}$	202.26	4	0.132	-	5.22
Benz(a)anthracene	BaA	C$_{18}$H$_{12}$	228.28	4	0.014	0.0001	5.91
Chrysene	Chr	C$_{18}$H$_{12}$	228.28	4	0.002	0.0002	5.91
Benzo(b)fluoranthene	B*b*F	C$_{20}$H$_{12}$	252.31	5	0.0012	0.0002	5.80
Benzo(k)fluoranthene	B*k*F	C$_{20}$H$_{12}$	252.31	5	0.0005	0.0002	6.00
Benzo(a)pyrene	B*a*P	C$_{20}$H$_{12}$	252.31	5	0.110	0.0002	6.04
Indeno(1,2,3-cd)pyrene	Ind	C$_{22}$H$_{12}$	276.33	6	0.062	0.0004	6.50
Dibenz (a,h)anthracene	DbA	C$_{22}$H$_{14}$	278.34	6	0.005	0.0003	6.75
Benzo (g,h,i) perylene	BPer	C$_{22}$H$_{12}$	276.33	6	0.0026	-	6.50

*Maximum Contaminant Level:
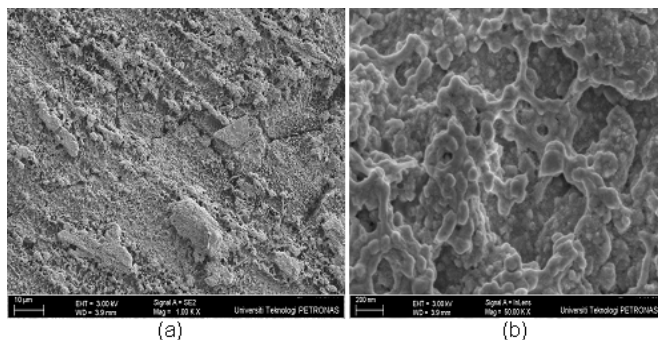
Figure 1. FESEM surface images of the Ti/IrO₂ anode with low (a) and high (b) magnifications.

Figure 2. EDAX of the Ti/IrO₂ anode surface

3. RESULTS AND DISCUSSION

3.1. Physical Characterization

Fig. 1(a) and 1(b) show the FESEM microstructure of Ti/IrO₂ electrode at low and high magnifications respectively. In Fig. 1(a), surface morphology of the thin film does not exhibit the cracked mud structure; it appeared to have a rough flat surface. Otogawa et al [31] found both flat and crack mud structures for IrO₂ coating. For oxygen evolution reaction both structures were found to exhibit good catalytic activity and dimensional stability [32]. In Fig. 1(b), nano-scale granular crystalline IrO₂ particles of size 44.3-165.1 nm are distributed on titanium surface. In Fig. 2, EDAX spectrum confirmed the presence of oxygen and iridium with weight % of 30.8 and 25.5 respectively. Fairly narrow and strong XRD diffraction peaks at angles of 28.11°, 35.00° and 40.19° suggested tetragonal crystalline IrO₂ shown in Fig. 3. Structure of coated surface depends upon concentration of coating material in precursor solution and temperatures of drying and calcination. In this study, precursor solution was easily dried at 100°C. Cracked mud structure is usually found when concentration of coated material is high or high temperature is used for drying. In case of Ti/Sb-SnO₂, it was assumed that cracked mud or porous surface can help in adsorption of OH radicals and organic matters [33]. However, researchers are focusing on the active coating materials for electrochemical degradation of organic pollutants in wastewater. The active coating enables the electrical charge transport between the base metal and the electrode/electrolyte interface. It must have high chemical and electrochemical stability and able to catalyze the desired electrochemical reaction. Comninellis and Vercesil [34] reported that IrO₂ used as doping material increased service life of anode. Comninellis [35] also proposed that mechanism of electrochemical oxidation of organic pollutant on IrO₂ anode was electrochemical selective oxidation while that on Ti/SnO₂ anode was electrochemical combustion.

3.2. Effect of pH and Electrolyte

Table 2 shows concentration of PAHs at initial pH 3, 6 and 9 without and with electrolyte. Initial pH of the solution was adjusted using molar solutions of sulfuric acid and sodium hydroxide. Results showed that naphthalene (2 benzene rings) was efficiently removed in both solutions without and with electrolyte (Fig. 4 and 5). PAHs with 3 and 4 benzene rings were completely degraded in the presence of electrolyte but not without. Fig. 4 shows complete
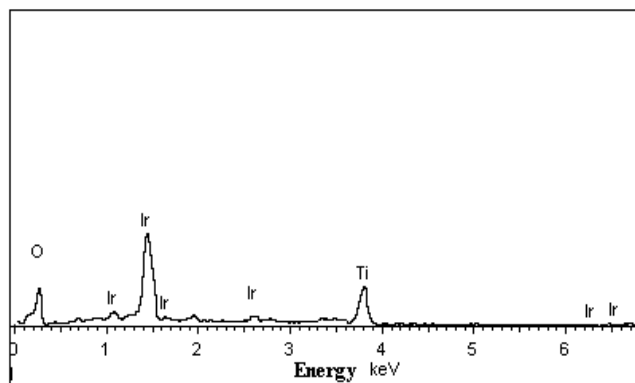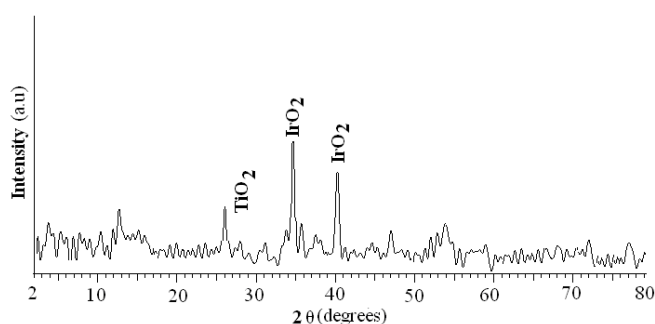

Figure 3. XRD pattern of Ti/IrO₂ anode surface

removal of Nap, Acy and Ace at pH3; Nap, Acy, Ace, Flu at pH6 and Nap, Acy, Ace, Flu, Phe, Ant, Fla and Pyr at pH9. Benzo(a)pyrene with 5 benzene rings was also completely removed in presence of electrolyte at initial pH values of 3 and 9. Overall concentrations of 5-6 rings PAHs decreases to trace level. Moreover 80 % of total PAHs were removed at all initial pH 3, 6 and 9 without using electrolyte; it shows the treatment was independent on pH.
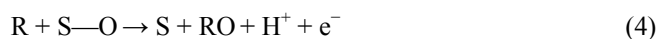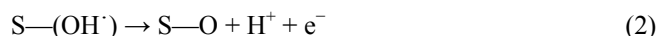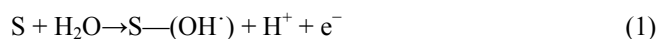
Among all initial pH conditions efficiency of oxidation of PAHs tends to increase at pH 9. Cañizares et al. [36] proposed that the pH does not influence the global oxidation rate even if initial oxidation rate was higher in basic media. Addition of NaCl as electrolyte suppresses the effect of pH on oxidation of PAHs. Up to 97 % total PAHs were removed at all initial pH 3, 6 and 9. This is due to indirect electrochemical oxidation of organic compounds takes place through chlorine/hypochlorite; however, the production rate of chlorine/hypochlorite was not affected by initial pH conditions. Vijayaraghavan et al. [37] reported that during the treatment of textile effluents, under fixed current density, the chlorine production was more or less the same, irrespective of the initial pH values (3.5-8.5). Electrolyte also increased the conductivity of solution and decreased cell voltage from 12 to 6 V.

3.3. Reaction mechanism

Mechanism for organic oxidation involves the formation of OH species produced from electrolysis of water (reaction (1)) or the

formation of higher oxides produced from electrochemical oxidation of the anode surface (reaction (2)). The higher oxides can also be decomposed into molecular oxygen (reaction (3)) through oxygen evolution reaction (OER) occurs. Some voltammetric studies show that some organic radicals (RO) are generated during electrooxidation of organic material like phenol which often tends to polymerize on electrode surface [38, 39]. These polymers present a low permeability and strongly adhere to the electrode surface, producing an insulating film that inhibits further oxidation of organic compounds.

Following reaction scheme was proposed as the mechanism for oxygen evolution and catalytic activity for organic degradation [38].
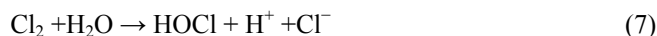
$$S + H_2O \rightarrow S\text{—}(OH^\cdot) + H^+ + e^- \tag{1}$$

$$S\text{—}(OH^\cdot) \rightarrow S\text{—}O + H^+ + e^- \tag{2}$$

$$S\text{-}O \rightarrow S + \frac{1}{2}O_2 \uparrow \tag{3}$$

$$R + S\text{—}O \rightarrow S + RO + H^+ + e^- \tag{4}$$

S stands for active sites on the oxide surface, R is organic content and S—(OH) and S—O are two adsorption intermediates or surface active species.

In reaction (5) chloride ion adsorbs and oxidizes on the active site (S) and reacts with either with chloride ion in solution (reaction (6)) or with another adsorbed chloride ion (reaction (7)) and liberates molecular chlorine [40]. The molecular chlorine reacts with OH ions to generate ClO⁻ ion (reaction (8)) and also react with water molecule to form hypocholorous acid (reaction (7)). These oxidants further help in oxidation of PAHs.

Following reaction scheme was proposed for chlorine evolution and indirect oxidation of organic compounds [40].

$$S + Cl^- \rightarrow S\text{—}Cl^- + e^- \tag{5}$$

$$Cl^- + S\text{—}Cl^- \rightarrow S + Cl_2 + 2e^- \tag{6}$$

$$2S\text{–}Cl^- \rightarrow 2S + Cl_2 \uparrow \tag{7}$$

$$Cl_2 + 2OH^\cdot \rightarrow Cl^- + ClO^- + H_2O \tag{6}$$

$$Cl_2 + H_2O \rightarrow HOCl + H^+ + Cl^- \tag{7}$$

$$HOCl \rightarrow H^+ + OCl^- \tag{8}$$

4. CONCLUSION

Ti/IrO₂ anode shows good electrocatalytic activity for PAHs degradation in both solutions (without and with electrolyte). PAHs containing 2 and 3 benzene rings can easily be oxidized in all the experimental condition tested. FESEM and XRD results support the presences of IrO₂ and its crystalline structure. The present study provides basis for future electrochemical studies on organics degradation at active anodes like Ti/IrO₂.

Table 2. Concentration before and after treatment without electrolyte and with electrolyte

PAHs	Retention Time (min)	Initial Concen. (μg/l)	Final Concen. (μg/l)					
			Initial pH					
			Without electrolyte			With electrolyte		
			3	6	9	3	6	9
Nap	7.57	10.69	0	0	0	0	0	0
Acy	11.19	9.41	0	0	0	0	0	0
Ace	11.61	9.90	0	0.33	0	0	0	0
Flu	12.84	8.04	0.22	0.75	0	0	0	0
Phe	15.12	8.60	0.7	1.02	0	0	0	0
Ant	15.13	7.34	0.56	1.1	0	0	0	0
Fla	17.96	7.67	0.82	1.77	0	0	0	0
Pyr	18.48	7.37	0.53	1.25	0	0	0	0
BaA	21.38	6.30	1.15	1.32	1.27	0.3	0.35	0.3
Chr	21.46	6.56	1.56	1.45	1.28	0.52	0.6	0.54
B*b*F	23.77	6.48	1.1	1.4	1.32	0.43	0.48	0.35
B*k*F	23.83	5.41	1.24	1.42	1.36	0.54	0.56	0.31
B*a*P	24.45	5.18	1.19	1.31	1.23	0	0.32	0
Ind	27.28	5.24	1.12	1.32	1.41	0.6	0.43	0.33
DbA	27.40	5.03	1.17	1.61	1.06	0.6	0.8	0.75
BPer	28.05	5.51	1.2	1.45	1.09	0	0.61	0
Total Concen.(μg/l)		114.73	12.56	17.50	10.02	2.99	4.15	2.58

Surface Characteristics of Ti/IrO₂ Anode Material and its Electrocatalytic Properties for Polycyclic Aromatic Hydrocarbons (PAHs) Degradation in Aqueous Solution / J. New Mat. Electrochem. Systems
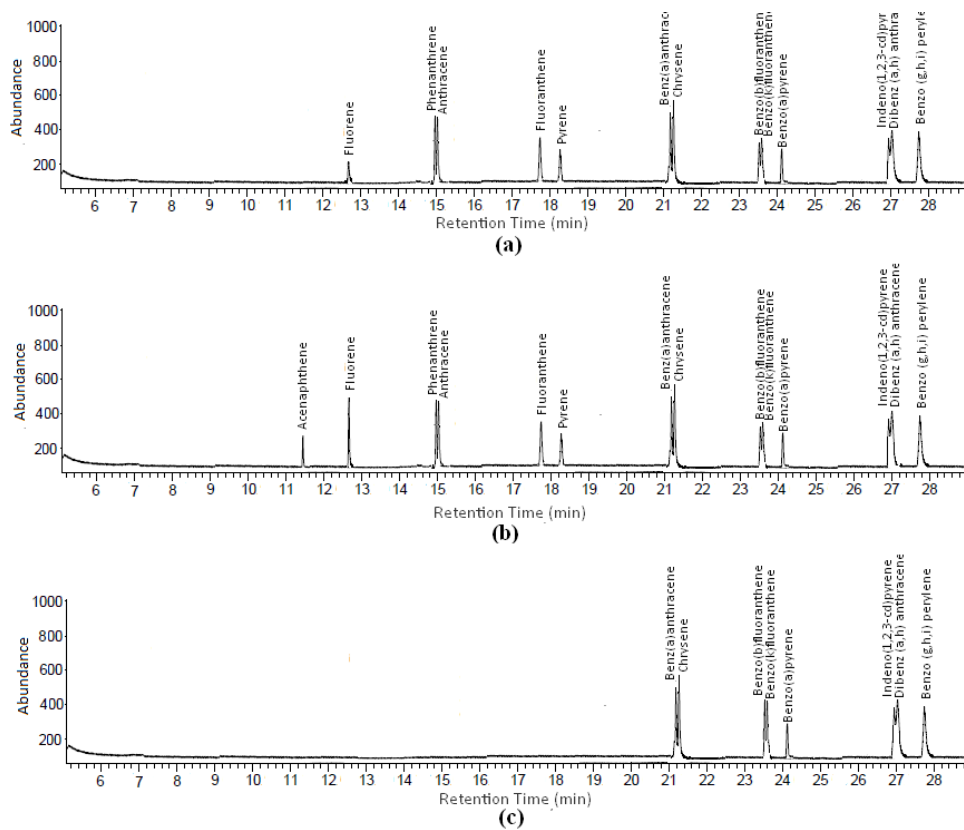
43

Figure 4. GC chromatograms for electrochemical removal of PAHs without electrolyte at (a) pH 3 (b) pH 6 (c) pH 9 in 4 h.
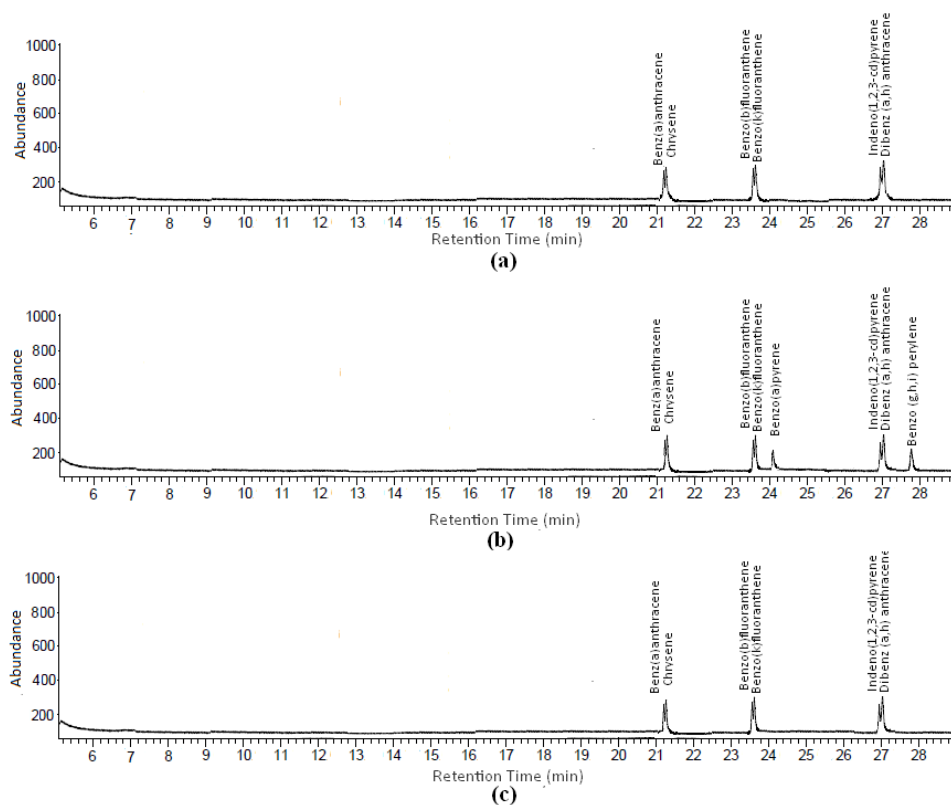

Figure 5. GC chromatograms for electrochemical removal of PAHs using electrolyte at (a) pH 3 (b) pH 6 (c) pH 9 in 4 h.

REFERENCES

[1] USEPA U, Integrated Risk Information System (IRIS). EPA; (1999).

[2] Agency for Toxic Substances and Disease Registry (ATSDR). Toxicological profile for polycyclic aromatic hydrocarbons (PAHs). August (1995). http://www.atsdr.cdc.gov/ToxProfiles/tp69.pdf

[3] USEPA. Standards and Regulations for Polycyclic Aromatic Hydrocarbons. http://www.atsdr.cdc.gov/csem/csem.asp?csem=13&po=8

[4] D. Mackay, W.Y. Shiu, K.C. Ma, Illustrated handbook of physical-chemical properties and environmental fate for organic chemicals: Polynuclear aromatic hydrocarbons, polychlorinated dioxins and dibenzofurans. Lewis Publishers, Chelsea, Michigan, USA (1992).

[5] E.N. Pakpahan, M.H. Isa, S.R.M. Kutty, S. Chantara, W. Wiriya, Environ. Tech., 34, 407 (2013).

[6] A. Chiavola, R. Baciocchi, R. Gavasci. J. Hazard. Mater., 184, 97 (2010).

[7] E.N. Pakpahan, M.H. Isa, S.R.M. Kutty, S. Chantara, J Sci. Ind. Res., 17, 430 (2012).

[8] O.S. Amodu, T.V. Ojumu and S.K.O. Ntwampe. Bioavailability of High Molecular Weight Polycyclic Aromatic Hydrocarbons Using Renewable Resources. http://dx.doi.org/10.5772/54727

[9] A. Yaqub, H. Ajab, M.H. Isa, H. Jusoh, M. Junaid, R. Farooq, J. New. Mater. Electrochem. Syst., 15, 289 (2012).

[10] A. Yaqub, H. Ajab, Rev. Chem. Eng., 29, 123 (2013).

[11] J. Kristóf, J. Mihály, S. Daolio, A. De Battisti, L. Nanni, C. Piccirillo, J. Electroanal. Chem., 434, 99 (1997).

[12] Y. Igarashi, K. Tani, M. Kasai, K. Ahikaga, T. Ito, Jpn. J. Appl. Phys., 39, 2083 (2000).

[13] F. Zhang, R. Barrowcliff, G. Stecker, W. Pan, D. Wang, S.T.J. Hsu, Appl. Phys., 44, 398 (2005).

[14] C.P. DePauli, S. Trasatti, J. Electroanal. Chem., 396, 161 (1995).

[15] N. Rajalakshmi, K.S. Dhathathreyan, Chem. Eng. J., 129, 31 (2007).

[16] Z. Yue, E. Yifeng, F. Louzhen, Q. Yongfu, Y. Shihe, Electrochim. Acta, 52, 5873 (2007).

[17] S. Fierro, A. Kapałka, C. Comninellis, Electrochem. Commun., 12, 172 (2010).

[18] A.A. El-Moneim, M.B. Mohamed, Electrochem. Sci., 7, 671 (2012).

[19] C. Comninellis, Electrochim. Acta, 39, 1857 (1994).

[20] L. Ouattara, T. Diaco, I. Duo, M. Panizza, G. Foti, C.J. Comninellis, Electrochem. Soc., 150, D41 (2003).

[21] X.Y. Li, Y.H. Cui, Y.J. Feng, Z.M. Xie, J.D. Gu. Water Res., 39, 1972 (2005).

[22] C.R. Costa, C.M.R. Botta, E.L.G. Espindola, P. Olivi, J. Hazard. Mater., 153, 616 (2008).

[23] A. Kapalka, G. Fóti, C. Comninellis, Electrochem. Commun., 10, 607 (2008).

[24] K.W. Kim, E.H. Lee, J.S. Kim, K.H. Shin, B.I. Jung. Electrochim. Acta, 47, 2525 (2002).

[25] C.L. Zanta, P.A. Michaud, C. Comninellis, A.R. De Andrade, J.F. Boodts, J. App. Electrochem., 33, 1211 (2003).

[26] N. Matyasovszky, M. Tian, A. Chen, The. J. of Phy. Chem. A, 113, 9348 (2009).

[27] R. Chaiyont, C. Badoe, C. Ponce de León, J.L. Nava, F.J. Recio, I. Sires, F.C. Walsh, Chem. Eng. Technol., 36, 123 (2013).

[28] M.P. Pechini, N. Adams, US Patent, 3 (1967) 3,330,697.

[29] EPA Methods. SW846 3510C, Separatory Funnel Liquid-Liquid Extraction. www.epa.gov/osw/hazard/testmethods/sw846/pdfs/3510c.pdf

[30] LUS. Standard operating procedure for oil spill source identification. "Water Extraction Procedure" LSU-RCAT SOP#001 – 08. Louisiana State University, page 1-10.

[31] R. Otogawa, M. Morimitsu, M. Matsunagab, Electrochim. Acta, 44, 1509 (1998).

[32] E.N. Balko, P.H. Nguyen, J. Appl. Electrochem, 21, 678 (1991).

[33] J.T. Kong, S.Y. Shi, X.P. Zhu, J.R. Ni, J. Environ. Sci., 19, 1380 (2007).

[34] C. Comninellis, and G.P. Vercesi, J. Appl. Electrochem., 21, 335 (1991).

[35] C. Comninellis, Electrochim. Acta. 39, 1857 (1994).

[36] P. Cañizares, C. Saez, J. Lobato, M.A. Rodrigo, Electrochim. Acta, 49, 4641 (2004).

[37] K. Vijayaraghavan, T.K. Ramanujam, N. Balasubramanian, Color Technol, 117, 49 (2001).

[38] X.M. Wang, J.M. Hu, J.Q. Zhang, C.N. Cao, Electrochim. Acta, 53, 3386 (2008).

[39] Z. Ežerskis, and Z. Jusys, J. Appl. Electrochem, 32, 543 (2002).

[40] J. Aromaa, O. Forsen, Electrochim. Acta, 51, 6104 (2006).